

Electronic structure of insulating Zr_3N_4 studied by resonant photoemission

P. Prieto,¹ A. Fernández,² L. Soriano,¹ F. Yubero,¹ and E. Elizalde,¹ A. R. González-Elipse,² and J. M. Sanz^{1,*}

¹*Instituto Universitario Nicolás Cabrera and Departamento de Física Aplicado C-XII, Universidad Autónoma de Madrid, Cantoblanco, E-28049 Madrid, Spain*

²*Instituto Ciencia de Materiales de Sevilla (Consejo Superior de Investigaciones Científicas—Universidad Sevilla), Departamento de Química Inorgánica, P.O. Box 1115, E-41071 Sevilla, Spain*

(Received 28 November 1994; revised manuscript received 9 March 1995)

The formation of insulating Zr_3N_4 by low-energy (5 KeV) N_2^+ bombardment of zirconium was studied by photoemission spectroscopy using synchrotron radiation. The electronic structure of Zr_3N_4 was then studied by resonant photoemission in the 32–80-eV photon-energy range. Resonance effects have been observed at ~ 41 and at ~ 50 eV, well above the Zr $4p$ binding energy (~ 29.5 eV) as measured by photoemission. The resonance at 41 eV is shown to be associated with the enhancement of those valence-band states with an important Zr $4d$ character. In fact, it has been used to isolate the cationic Zr $4d$ contribution to the valence band of Zr_3N_4 . Furthermore, we have identified those regions of the valence band with a predominant N $2p$ character by direct photoemission at $h\nu \geq 70$ eV for which the Zr $4d$ photoemission cross section is negligible. A broad resonance at $h\nu = 50$ eV seems to be caused by resonant processes involving N $2p$ states, however, the exact mechanism implicated remains unknown.

The synthesis of nitrogen-rich zirconium nitrides (i.e., ZrN_x , with $x > 1$) using methods based on low-energy ion beams has been reported by several authors.^{1–4} In fact, a new dielectric phase, optically transparent and electrically insulating, was reported for zirconium and hafnium with compositions close to Zr_3N_4 and Hf_3N_4 , respectively, but not for titanium.¹ However, and in spite of their interesting characteristics, the number of both theoretical and experimental studies regarding this phase has been very low.^{1–4}

In the present study we use resonant photoemission spectroscopy to study the valence band of Zr_3N_4 . RPES is, in fact, a well-established method^{5–12} for determining the cationic character of specific regions of the occupied density of states.

Polycrystalline Zr foil 25 μm thick from Goodfellow Metals was used as a target in this study. Low-energy N_2^+ bombardment of the zirconium sample was performed with a Penning-type ion gun. The current density was $\approx 0.42 \mu\text{A}/\text{cm}^2$, that is, 2.63×10^{12} ions/ $\text{cm}^2 \text{s}$. The energy of the N_2^+ ions was kept at 5 KeV, which in fact corresponds to 2.5-KeV atomic ions.

The photoemission experiments were performed with synchrotron radiation from the LURE beam line SA71. Photon energies in the range $32 \leq h\nu \leq 80$ eV were used. Normal emission spectra were recorded with an angle-resolved electron energy analyzer. The angle of incidence of the light was 67.5° with respect to the sample normal.

Figure 1 shows electron distribution curves (EDC's) for the valence-band region of zirconium as a function of the N_2^+ (5 KeV) fluence and the average composition ZrN_x , as labeled. The spectra were measured at a photon energy of $h\nu = 43$ eV and have been depicted after normalization to the flux of incident photons. The most significant effects to be observed are the growth of a broad emission band at energies between 3 and 8 eV and the continuous decrease of the band at the Fermi level until it is completely suppressed for a N_2^+ fluence above 10^{16} ions/ cm^2 .

The results of Fig. 1 are qualitatively easy to under-

stand as a transfer of electrons from the d band at the Fermi level to available N $2p$ states at higher binding energies as the nitrogen concentration x (i.e., ZrN_x) increases during the implantation process.^{13,14} In fact, this simple picture has been quantitatively analyzed in a previous work,⁴ where a complete analysis of both the valence-band and core-level XPS spectra showed that the density of electrons per atom of zirconium associated with the d band (n_d) depends linearly on x according to the formula $n_d = 4 - 3x$, giving $n_d = 0$ (i.e., a complete suppression of the d band) for $x = 1.33$ (i.e., Zr_3N_4).⁴ In the present case, we used the above relationship to estimate the average composition of the nitride by a simple quantification of the d band for every N_2^+ fluence in terms of the valence band of metallic zirconium. The results have been included as a label in Fig. 1. Obviously, the spectrum labeled $ZrN_{1.33}$ corresponds to the one where the d band has been completely depopulated.⁴ In general, this behavior is well known in substoichiometric nitrides (i.e., ZrN_x),¹⁵ with x in the range of $0.5 \leq x \leq 1$. Nevertheless, the most spectacular effects of the complete depopulation of the d band at the Fermi level and the opening of an energy gap of ~ 1.6 eV for $x \approx 1.33$ have not been shown previously.

Figure 1 also shows that upon N_2^+ bombardment, the N $2p$ band also undergoes some shape changes, mainly around 3.3 eV. The valence band undergoes a certain broadening for stoichiometries close to ZrN and becomes sharper when the insulating Zr_3N_4 is formed. Interestingly, the maximum of the valence band at 4.9 eV remains nearly constant for the stoichiometries represented in Fig. 1.

Figure 2 shows the valence band of Zr_3N_4 measured at different photon energies between 33 and 70 eV after normalization to the flux of incident photons and subtraction of the background arising from secondary electrons.¹⁶ From this figure we can estimate a valence-band-width (i.e., energy separation between the points of maximum slope on each side of the band) of approximately 5 eV.

Furthermore, we can locate the edge of the valence band at 1.6-eV binding energy (i.e., by extrapolating the tangent to the low-binding-energy side of the N $2p$ band until it crosses the energy axis) which is consistent with the value determined by XPS (Ref. 4) and the optical gap of 2.2 eV published in the literature.¹ However, the most interesting information of all to be found in this figure is the effect produced by changing the photon energy on the intensity and the shape of the valence band. The results clearly demonstrate that it is caused by a typical resonant photoemission process of a constant binding-energy feature.¹⁷ Any explanation in terms of a superposition of a photoemission signal with Auger-like features (constant kinetic energy) involving the N_1 level (i.e., $N_1N_{23}N_{45}$ and $N_1N_{45}N_{45}$ at ≈ 20 - and ≈ 55 -eV kinetic energy, respectively) can be disregarded.

The resonance process is qualitatively explained as being due to the creation of an excited state $[4p^54d^1]^*$ when the photon energy is swept over Zr $4p \rightarrow 4d$ excitation energy. This excited state remains localized in the cation and relaxes along an intra-atomic direct recombination process to the same final state as the conventional photoemission of an electron from the valence band.¹⁷ The interference between those two processes (i.e., photoemission and direct recombination), which produce the same final state, is then the cause of the resonant enhancement of the d states. Although the required localization of the excited state could be questioned for the $4d$ wave functions involved here, the experimental observation of resonant photoemission and even of autoionization emission in electron-impact emission experiments on pure Zr and zirconium compounds (e.g., ZrO_2 , ZrN, and ZrCu) (Refs. 6–8 and 18) clearly confirm that the conditions of the localization have to be relaxed to include wave functions of more extended nature. In the case Zr_3N_4 with a nominal $Zr^{4+} 4d^0$ configuration, the decay of the excited state is only possible by energy transfer to

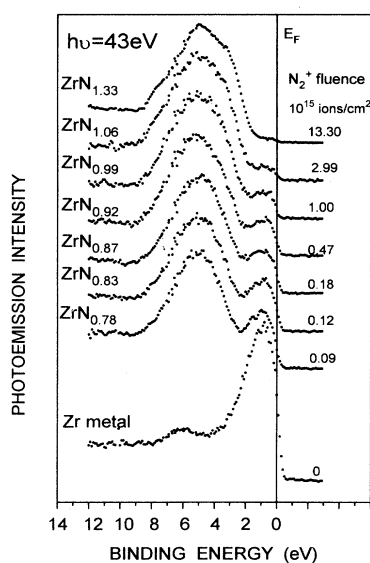


FIG. 1. Valence-band photoemission spectra at $h\nu=43$ eV from Zr and ZrN_x obtained by bombardment with 5-KeV N_2^+ ions at increasing fluence (see text for details on the determination of x).

those electrons involved in the valence band through Zr $4d-N 2p$ hybridization. In this way RPES can be used to isolate those regions of the valence band with a significant d character.^{5,6,9,11,12}

Figure 3 shows the integrated intensity of the whole N $2p$ emission band for Zr_3N_4 [Fig. 3(a)] together with the respective intensities at 3.3- and 4.9-eV binding energies [Fig. 3(b)] directly measured from the spectra of Fig. 2. In addition the EELS spectrum corresponding to the Zr $4p$ core excitations has been included in Fig. 3(a) for comparison. The total intensity of the valence band exhibits a rather sharp rise up to $h\nu=41$ eV, followed by a broad feature which peaks at $h\nu=50$ eV, after which there is a gradual falloff for higher photon energies. This behavior is also followed by the intensities at 3.3 and 4.9 eV [cf. Fig. 3(b)]. However, while the states at 4.9 eV show their maximum enhancement at 41 eV and a shoulder at 50 eV, the profile of the states at 3.3 eV shows a shoulder at 41 eV and maximizes at a photon energy of 50 eV.

Figure 3(a) clearly shows that the intensity enhancement observed at $h\nu=41$ eV is consistent with the Zr $4p \rightarrow 4d$ core excitations of Zr_3N_4 as observed by electron-energy-loss spectroscopy (i.e., EELS). Conversely, at energies above 41 eV the EELS spectrum does not show any distinguishable feature which could be associated with the broad resonance around 50 eV. The broad feature at ~ 60 eV in the EELS spectrum corresponds to the ionization of the Zr $4s$ atomic level¹⁸ and can be ignored in the present study.

The resonance at $h\nu=41$ eV can thus be accounted for by the Zr $4d$ contribution to the valence band, although it is well above (~ 11.5 eV) the expected $4p \rightarrow 4d$ threshold at 29.5 eV (i.e., the binding energy of Zr $4p$) as measured by photoemission (cf. Fig. 2). Similar delays between the

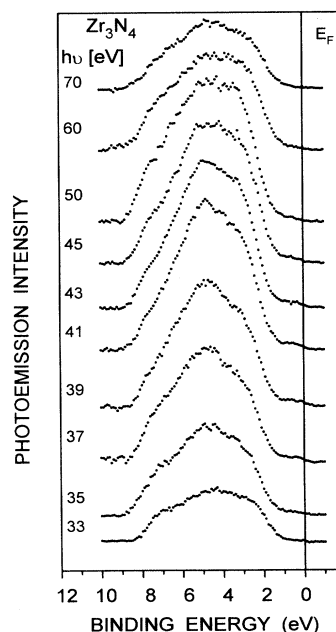


FIG. 2. Valence-band spectra of Zr_3N_4 measured at various photon energies, showing the resonant behavior.

threshold and resonance have been observed in Zr (~ 10 eV) (Ref. 8) and zirconium compounds like ZrO_2 (~ 8 eV) (Refs. 6, 18, and 19) and ZrN (~ 10 eV),⁷ and seem to be commonly observed in transition metals and their compounds with less than half-filled d orbitals.^{17,20}

In order to follow in a more meaningful way the changes observed in the valence band as a function of the photon energy, we generated difference spectra. Figure 4 shows the difference spectra obtained by subtracting the spectrum measured at $h\nu=35$ eV (off-resonance) from those measured at $h\nu=40, 42, 45,$ and 50 eV. For comparison the valence band of Zr_3N_4 measured by XPS (i.e., $h\nu=1253.6$ eV) (Ref. 4) has also been depicted. It is interesting to observe that the (40–35)-difference spectrum agrees remarkably well with the valence band measured by XPS. Considering that the XPS valence band is a good representative of the occupied states with a predominant d character (i.e., for $h\nu=1253.6$ eV, the cross section of the Zr $4d$ states is ten times greater than for the N $2p$ states²¹), the above-mentioned agreement confirms that the resonance at energies around 41 eV is caused by the enhancement of the Zr $4d$ states involved in the valence band of Zr_3N_4 . Therefore, we conclude that the (40–35)-difference spectrum reproduces those regions of the valence band with a significant d character. Furthermore it provides clear evidence that the maximum admixture of Zr $4d$ orbitals is located at 4.9-eV binding energy, which also explains the fact that the states at 4.9 eV maximize its intensity at $h\nu=41$ eV [cf. Fig. 3(b)].

The difference spectra depicted in Fig. 4 also show that although the intensity enhancement manifests itself along the whole valence band, there is a gradual relative enhancement of the states at the low-binding-energy side (i.e., 3.3 eV) with respect to those states at 4.9 eV, as the photon energy is increased from 40 to 50 eV. For the (50–35)-difference spectrum it is observed that the maximum at 4.9 eV has disappeared, and the spectrum becomes more squarelike as a consequence of the relative enhancement of the intensity around ~ 3.3 eV and above 7 eV with respect to the maximum at ~ 4.9 eV.

In regard of the enhancement observed at $h\nu=50$ eV, which cannot be associated with the Zr $4d$ states, a clear explanation is not yet available. In fact, although extra resonances not related to the d states derived from the metal have been previously observed in other compounds (e.g., TiO_2 , MoS_2 , and ZrO_2),^{9,11,12,19} their origin appears rather controversial. Assuming a purely intra-atomic direct recombination mechanism the resonance should be considered to be caused by other cationic contributions (i.e., s states) to the valence band.^{11,12} However, the observed enhancement results difficult to explain quantitatively only in terms of the cationic-derived s states, as in general they contribute very weakly to the valence band and are usually neglected.

If we disregard an explanation in terms of states derived from the cation, we still can consider resonance effects involving N $2p$ states. In fact, although it contradicts the essential assumption of RPES that the direct recombination mechanism is purely intra-atomic, inter-atomic deexcitation mechanisms involving O $2p$ states have been invoked to explain resonance effects in Ti_2O_3

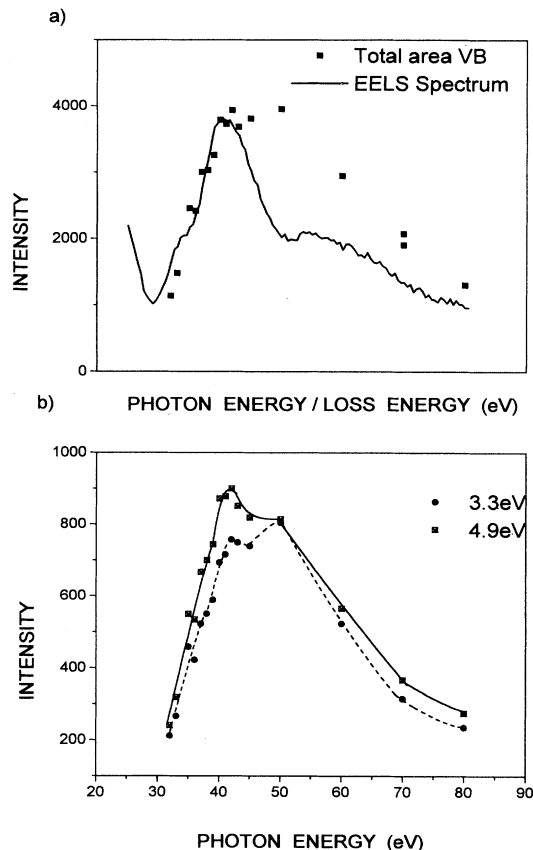


FIG. 3. (a) Photon-energy dependence of the total area of the valence band of Zr_3N_4 (■). The $4p$ core losses as measured by EELS (line) are also included. (b) CIS curves obtained from the spectra of Fig. 2, corresponding to different parts of the valence band at 3.3 (●) and 4.9 eV (□).

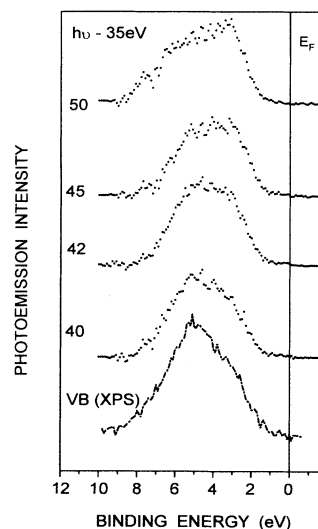


FIG. 4. Difference curves calculated by subtraction of the spectrum measured at 35 eV from the spectra measured at different photon energies, as labeled (cf. Fig. 2). The valence band of Zr_3N_4 obtained by XPS (Ref. 4) has been included for comparison.

and V_2O_3 .¹⁰ More recently, a study of photoemission resonance effects in ZrO_2 shows that the enhancement of the valence band associated with an extra broad resonance at photon energies around 50 eV is in good agreement with the O 2*p* density of states.¹⁹ In the present case of Zr_3N_4 a reliable N 2*p* density of states is not available for comparison. However, taking into account that at photon energies ≥ 70 eV the photoemission cross section for N 2*p* states is an order of magnitude greater than for Zr 4*d*, the spectra measured at 70 and 80 eV can be considered good representatives of the N 2*p* component of the valence band. In fact the Cooper minimum for Zr 4*d* is expected at ~ 80 eV.²¹ The comparison between the (50–35)-difference spectrum (cf. Fig. 4) and the valence band measured at $h\nu=70$ eV (cf. Fig. 2) shows an overall good agreement and therefore supports the idea that the N 2*p* states themselves resonate when the photon energy is tuned at 50 eV. In this case, the mechanism would be nonlocal and probably involve final states which are not intrinsically localized, but the details and the exact mechanism implicated in the process remain unknown. The N 2*p* character of the states at 3.3 eV can also be inferred from previous experiments,⁴ where it was shown that their appearance in the valence-band spectrum of ZrN_x is closely associated with the use of low-energy N_2^+ ions and the formation of the insulating nitride (i.e., Zr_3N_4) by N_2^+ bombardment (cf. Fig. 1). Excess of nitrogen seems to be necessary to create the states at 3.3 eV in the N 2*p* band, which finally allow the location of all the *d* electrons of zirconium, so that Zr_3N_4 becomes an insulator. Nevertheless, a better understanding of those changes which significantly affect the electrical and optical properties of the nitride requires a full characterization of the crystal structure and a comparison with theoretical calculations. However, a comparison with theoretical predictions is not possible at present, because reliable band-structure calculations of Zr_3N_4 are not available. The only published energy-band-structure calculation was

performed by Schwarz *et al.*³ for Zr_3N_4 and corresponding compounds of titanium and hafnium using the augmented-spherical-waves method. Nevertheless, this calculation was unable to predict the insulating behavior of Zr_3N_4 and Hf_3N_4 .

In conclusion, the electronic changes induced by 5-keV N_2^+ ions in zirconium were studied by PES using synchrotron radiation. It was shown that upon 5-keV N_2^+ bombardment it is possible to form an insulating nitride which according to a previous quantitative XPS analysis⁴ is assigned to Zr_3N_4 . The data provide a clear visualization of the localization of all the valence electrons within the N 2*p* band and the opening of a gap of ~ 1.6 eV at the Fermi level when the nitrogen content *x* in ZrN_x reaches 1.33 (i.e., Zr_3N_4). In addition, we performed a RPES study of the valence band of Zr_3N_4 in the 32–80-eV photon-energy range. Strong resonance effects were found all along the valence band. More specifically, for the total intensity of the N 2*p* valence band, we found a resonance profile that peaked at ~ 41 eV, which is associated mainly with the enhancement of the Zr 4*d* contribution to the valence band. Whereas that resonance has been used to isolate the Zr 4*d* contribution to the valence band of Zr_3N_4 , the corresponding N 2*p* density of states has been estimated directly by measuring valence-band spectra at photon energies around 70–80 eV. It is shown that the Zr 4*d* states hybridize significantly with the N 2*p* orbitals, contributing considerably, but not uniformly, along the whole valence band of Zr_3N_4 . A broad resonance observed at ~ 50 eV is tentatively assigned to resonant processes involving the N 2*p* states, although the exact mechanism remains unexplained.

This study has been supported by the CICYT and DGICYT of Spain under Contract Nos. MAT93/0805, URC 27/93, and PB93-0240, and by the European Union within the Human Capital and Mobility program under Contract No. ERBCHRXCT 930358.

*Author to whom all correspondence should be sent.

¹B. O. Johansson *et al.*, *J. Mater. Res.* **1**, 442 (1986).

²B. O. Johansson *et al.*, *Appl. Phys. Lett.* **44**, 670 (1984).

³K. Schwarz *et al.*, *Phys. Rev. B* **32**, 8312 (1985).

⁴P. Prieto *et al.*, *Phys. Rev. B* **47**, 1613 (1993); P. Prieto, Ph.D. thesis, Universidad Autónoma de Madrid, 1992.

⁵R. Courths *et al.*, *Solid State Commun.* **70**, 1047 (1989).

⁶J. M. Sanz *et al.*, *Surf. Sci.* **307/309**, 848 (1994).

⁷R. D. Bringans and H. Höchst, *Phys. Rev. B* **30**, 5416 (1984).

⁸C. G. H. Walker *et al.*, *Solid State Commun.* **82**, 573 (1992).

⁹R. Heise *et al.*, *Solid State Commun.* **84**, 599 (1992).

¹⁰K. E. Smith and V. E. Henrich, *Phys. Rev. B* **38**, 9571 (1988).

¹¹Z. Zhang *et al.*, *Phys. Rev. B* **43**, 12 004 (1991).

¹²J. R. Lince *et al.*, *Phys. Rev. B* **43**, 4641 (1991).

¹³H. Höchst *et al.*, *Phys. Rev. B* **25**, 7183 (1982).

¹⁴A. Callenas *et al.*, *Phys. Rev. B* **30**, 635 (1984).

¹⁵L. Porte, *Solid State Commun.* **50**, 303 (1984).

¹⁶D. A. Shirley, *Phys. Rev. B* **5**, 4709 (1972).

¹⁷L. C. Davis, *J. Appl. Phys.* **59**, R25 (1986).

¹⁸J. M. Sanz and C. Palacio, *Solid State Commun.* **64**, 189 (1987).

¹⁹C. Morant, A. R. Gonzalez-Elipse, A. Fernández, L. Soriano, A. Stampf, A. M. Bradshaw, and J. M. Sanz (unpublished).

²⁰J. L. Dehmer *et al.*, *Phys. Rev. Lett.* **26**, 1521 (1971).

²¹J. J. Yeh and I. Lindau, *At. Data Nucl. Data Tables* **32**, 1 (1985).